

EMISSION LINE PROPERTIES FROM BROAD-BAND PHOTOMETRY: IMPACT ON SELECTION AND PHYSICAL PARAMETER ESTIMATION

S. de Barros¹, H. Nayyeri¹, N. Reddy¹ and B. Mobasher¹

Abstract. Several works have now shown that nebular emission can have a significant impact on broad-band photometry of high-redshift galaxies ($z > 3$), and how this can affect parameter estimation from SED fitting. While relatively small spectroscopic samples have been used to estimate this impact, we here focus on a large spectroscopic sample ($N \sim 2300$) at $z \sim 2$, with measured $H\alpha$ fluxes for ~ 100 galaxies. Under appropriate assumptions, our SED fitting code is able to reproduce observed $H\alpha$ fluxes, and we infer that $\sim 20\%$ of our sample have parameters significantly affected when nebular emission is taken into account.

We also determine how nebular emission can affect selection and parameter estimation of evolved galaxies (Balmer Break galaxies) at high-redshift ($z \sim 4$).

Keywords: galaxies: starburst galaxies: high redshift galaxies: evolution galaxies: star formation

1 Introduction

Although nebular emission (i.e. emission lines and nebular continuous emission from HII regions) is ubiquitous in regions of massive star formation, strong or dominant in optical spectra of nearby star forming galaxies, and present in numerous types of galaxies, its impact on the determination of physical parameters of galaxies, in particular at high redshift, has been neglected until recently (cf. overview in Schaerer & de Barros 2011).

The analysis of samples of $z \sim 6-8$ and $z \sim 3-6$ LBGs observed with *HST* and *Spitzer* further demonstrates the potential impact of nebular emission on the physical parameters derived from SED fits of high- z galaxies (Schaerer & de Barros 2010; de Barros et al. 2012; Schaerer et al. 2013). It has now become clear (Schaerer & de Barros 2009, 2010; Ono et al. 2010; Lidman et al. 2012) that nebular emission (both lines and continuum emission) must be taken into account for the interpretation of photometric measurements of the SEDs of star-forming galaxies at high- z . In parallel, diverse evidence of strong emission lines galaxies with strong emission lines and/or strong contributions of nebular emission to broad-band fluxes has been found at different redshifts, e.g. by Shim et al. (2011); McLinden et al. (2011); Atek et al. (2011); Trump et al. (2011); van der Wel et al. (2011); Labbe et al. (2012); Stark et al. (2013); Smit et al. (2013). Unfortunately, at redshift as high as $z \sim 3$, direct measurement of emission lines remains a difficult task with current facilities, while some results at $3.0 < z < 3.8$ are encouraging (e.g. Schenker et al. 2013).

The main idea of this work is to use a spectroscopic sample at $z \sim 2$ (Erb et al. 2006), where measurements of emission lines ($H\alpha$) are already available for a significant subsample. This subsample is used to test the ability of our SED fitting code (but the results can be generalized to any SED fitting code accounting for nebular emission) to reproduce properly observed emission lines, under different assumptions. Once our code calibrated, we infer the impact of nebular emission on parameter estimation. In parallel, we also determine how nebular emission can affect selection and physical parameter estimation of evolved galaxies at $z \sim 4$ (Nayyeri et al. 2013). We adopt a Λ -CDM cosmological model with $H_0=70$ km s⁻¹ Mpc⁻¹, $\Omega_m=0.3$ and $\Omega_\Lambda=0.7$. All magnitudes are expressed in the AB system (Oke & Gunn 1983).

¹ Department of Physics and Astronomy, University of California, Riverside, 900 University Avenue, Riverside, CA 92521, USA

2 SED fitting code

We use a recent, modified version of the Hyperz photometric redshift code of Bolzonella et al. (2000), taking into account nebular emission (lines and continua). We consider a large set of spectral templates (Bruzual & Charlot 2003), covering different metallicities and a wide range of star formation (SF) histories (exponentially decreasing, constant and exponentially rising SF), and we add the effects of nebular emission following the method presented in Schaerer & de Barros (2009, 2010). We account for attenuation from the intergalactic and the interstellar medium. With these assumptions we fit the observed SEDs by straightforward least-square minimization.

In practice we adopt a spectral templates computed for a Salpeter IMF (Salpeter 1955) from 0.1 to 100 M_{\odot} , and we properly treat the returned ISM mass from stars. Nebular emission from continuum processes and lines is added to the spectra predicted from the GALAXEV models as described in Schaerer & de Barros (2009), proportionally to the Lyman continuum photon production. The relative line intensities of He and metals are taken from Anders & Fritze-v. Alvensleben (2003), including galaxies grouped in three metallicity intervals covering $\sim 1/50$ – $1 Z_{\odot}$. Hydrogen lines from the Lyman to the Brackett series are included with relative intensities given by case B. For galactic attenuation we use the Calzetti law (Calzetti et al. 2000). The IGM is treated following Madau (1995).

We test two attenuations, one applying the same attenuation to the stellar and nebular emission, and the other following Calzetti (1997), who find a more important attenuation for nebular emission in comparison with stellar emission, with $E(B - V)_{*} = 0.44 \times E(B - V)_{neb}$.

3 Data

Galaxies at redshifts $1.4 \leq z \leq 3.7$ were selected using the BM, BX, and Lyman-break galaxy (LBG) rest-UV color criteria (Steidel et al. 2003, 2004; Adelberger et al. 2004). The imaging data were obtained mostly with the Palomar Large Format Camera or the Keck Low Resolution Imaging Spectrograph (Oke et al. 1995; Steidel et al. 2004). The photometry and spectroscopic follow-up for this survey are described in Steidel et al. (2003, 2004); Adelberger et al. (2004). To probe the strength of the Balmer break in $z \sim 2$ galaxies, we used J and/or Ks imaging (Palomar/WIRC and Magellan/PANIC). We also used Spitzer/IRAC data. The IRAC coverage of our galaxies typically included either channels 1 ($3.6 \mu\text{m}$) and 3 ($5.8 \mu\text{m}$) or channels 2 ($4.5 \mu\text{m}$) and 4 ($8.0 \mu\text{m}$), with a small fraction of galaxies having coverage in all four channels. Additionally, for a small fraction of this $z \sim 2$ sample, we obtained (HST)/WFC3-F160W (H band) data.

The search and characterization of evolved galaxies at $z \sim 4$ has been done with Wide Field Camera 3 (WFC3) near Infra Red observations in the GOODS-S field performed as a part of the CANDELS project. The U-band data in the GOODS-S area were taken using the VIMOS instrument on Very Large Telescope. Optical data comes from HST/ACS, with F435W, F606W, F775W and F850LP filters. Near-infrared observations are in the F098M and F105W filters with the former one being used for the GOODS-S ERS, F125W and F160W. GOODS-S has also observations by the VLT HAWK-I Ks filter at effective wavelength of $2.2 \mu\text{m}$. Finally, we also use Spitzer/IRAC data in all four channels (for a detailed description of the data, see Nayyeri et al. 2013, and references therein).

4 Physical parameters of $z \sim 2$ star-forming galaxies

First, we test the ability of the three star formation histories (exponentially declining/rising, and constant) used here, to reproduce observed $\text{H}\alpha$ fluxes, since these different histories lead to different prediction of line strength (de Barros et al. 2012; Schaerer et al. 2013). Only declining SFH is unable to reproduce observed fluxes, leading to lower $f(\text{H}\alpha)_{\text{SED}}$ in comparison with $f(\text{H}\alpha)_{\text{obs}}$. In Figure 1, we show the result with a rising SFH (similar results with a constant SFH). While different attenuation between nebular and stellar emission seems physically motivated, our results clearly show that applying the same differential attenuation than Calzetti (1997) leads overall to underpredict $\text{H}\alpha$ fluxes (Figure 1, right), while for some individual objects, this leads to improve the correlation between observed and predicted $\text{H}\alpha$ fluxes. Similarly, Kashino et al. (2013) find that the Calzetti (1997) relation evolves at higher redshift, which may indicate a more uniform dust distribution in high- z galaxies as compared to local galaxies.

We also test SED fitting with a lower age limit (> 50 Myr), to avoid conflict between dynamical timescale and age. Using this limit improve marginally the agreement between predicted and observed fluxes.

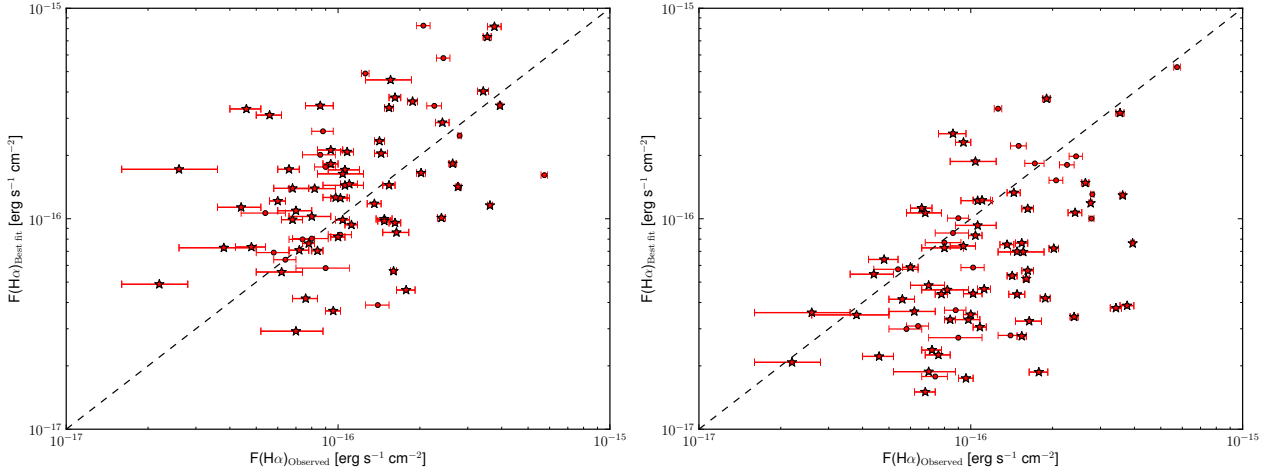


Fig. 1. Left: $H\alpha$ fluxes inferred from best-fit SED fitting vs observed $H\alpha$ fluxes, with a rising SFH, applying the same attenuation to the stellar and nebular emission. **Right:** same but with a differential attenuation (Calzetti 1997). Red stars: galaxies with $H\alpha$ falling in one filter (F160 or K band), red dots: galaxies with $H\alpha$ line falling in no filter.

Relying on our consistency test between predicted and observed $H\alpha$ flux, we use only rising (since constant leads to similar results) SFH, with similar attenuation between stellar and nebular emission, to infer physical properties of our $z \sim 2$ sample, and determine how nebular emission affects parameter estimation. The main parameter expected to be affected by nebular emission is age (Schaerer & de Barros 2009), since some lines ($H\beta$, [OIII] doublet, [OII]) can mimic a Balmer break. We compare results of our fit without and with nebular emission, and we find that 468 galaxies (20% of our sample) have $\log(\text{Age}) - \log(\text{Age}_{\text{NEB}}) \geq 0.3$.

At $z \sim 2$, stellar masses are strongly constrained by IRAC data, since no strong emission lines fall in these filters. However, the stellar mass estimation can be affected by nebular emission if age is significantly affected too, since the mass to light ratio evolves with age. Indeed, in Figure 2, we show the comparison between stellar mass estimated without nebular emission (M_{\star}) and stellar mass estimated with nebular emission ($M_{\star\text{NEB}}$), for galaxies for which age estimation changes when accounting for nebular emission ($\log(\text{Age}) - \log(\text{Age}_{\text{NEB}}) \geq 0.3$). The impact of nebular emission is however not very strong since we find only 293 galaxies (12% of the sample) with $\log(M_{\star}) - \log(M_{\star\text{NEB}}) \geq 0.3$

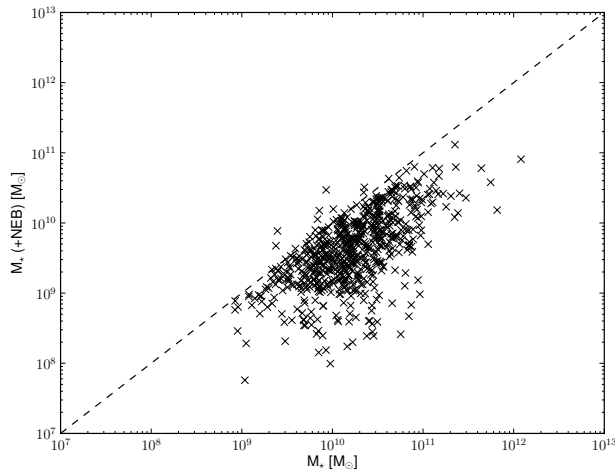


Fig. 2. Stellar mass estimated without nebular emission vs stellar mass estimated with nebular emission for galaxies with $\log(\text{Age}) - \log(\text{Age}_{\text{NEB}}) \geq 0.3$. The dashed is the one to one relation.

In another paper, we will present detailed results and implications for star formation history.

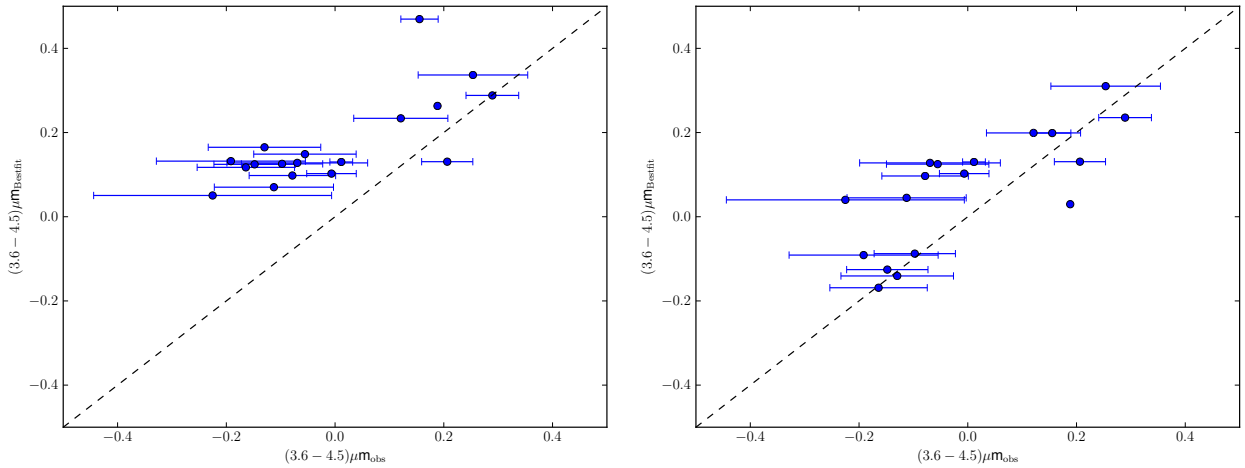


Fig. 3. Left: $(3.6-4.5)\mu\text{m}$ observed color vs $(3.6-4.5)\mu\text{m}$ best-fit SED color for objects with $3.8 < z_{\text{phot}} < 5.0$, without taking into account nebular emission. **Right:** same but accounting for nebular emission.

5 Selection and physical properties of evolved galaxies at $z \sim 4$

Using evolutionary tracks, we define a color-color selection to identify evolved galaxies at $z \sim 4$, i.e. with a strong Balmer break (see Nayyeri et al. 2013, for selection criteria). Contamination is mainly due to dusty starburst galaxies, while nebular emission can allow low-redshift starburst to pass the selection in narrow ranges of redshift, when flux in selection filters is enhanced by some emission lines.

The physical properties of $z \sim 4$ galaxies are more strongly affected by nebular emission in comparison with $z \sim 2$ galaxies, since strong emission lines (e.g. $\text{H}\alpha$) affect IRAC fluxes at $z > 3.8$. While no current facilities allow direct measurements of emission lines (except $\text{Ly}\alpha$) at those redshift, $\text{H}\alpha$ line is found in the $3.6\mu\text{m}$ filter at $3.8 < z < 5.0$, whereas very few lines are expected in the $4.5\mu\text{m}$ filter. Excess in the $3.6\mu\text{m}$ filter is interpreted as an additional flux due to the $\text{H}\alpha$ line, and the $(3.6-4.5)\mu\text{m}$ color is basically a model independent measurement of the $\text{H}\alpha$ strength (Shim et al. 2011; de Barros et al. 2012; Stark et al. 2013). In Figure 3, we show the ability of our SED fitting code to reproduce observed $(3.6-4.5)\mu\text{m}$ color of objects identified as evolved galaxies. As at $z \sim 2$, we show that our SED fitting code provide fits consistent with the observed strength of $\text{H}\alpha$.

SED fitting of our complete sample of evolved galaxies shows that an upper limit of $\sim 20\%$ of the sample show contamination by emission lines, which affects age, stellar mass, dust and star formation rate estimation. Typically, ages are reduced, stellar masses decreased, and dust attenuation and SFR increased. The complete analysis of these evolved galaxies can be found in (Nayyeri et al. 2013).

6 Conclusions

We present an homogeneous study of a sample of 2389 star-forming galaxies at $z \sim 2$, all spectroscopically confirmed, with deep photometry from up to $8\mu\text{m}$. We also use available measurement of $\text{H}\alpha$ line for ~ 100 galaxies. Using a modified version of the *HyperZ* photometric redshift code which takes into account nebular emission (Schaerer & de Barros 2009), we explore a range of star formation history (constant, exponentially decreasing and rising). We test different star formation histories and differential attenuation between stellar and nebular emission (Calzetti 1997) to reproduce observed $\text{H}\alpha$ fluxes. Declining SFH is unable to provide consistent $f(\text{H}\alpha)_{\text{SED}}$, while differential attenuation leads also to underestimated $f(\text{H}\alpha)_{\text{SED}}$ in comparison with observed fluxes. The main parameter affected by nebular emission is age, since some lines can mimic a Balmer break (Schaerer & de Barros 2009, 2010). While stellar mass is strongly constrained by IRAC data, changes in age estimation also affects significantly stellar mass estimation for a fraction of our sample (12%).

At $z \sim 4$, the characterization of evolved galaxies is more affected when nebular emission is accounted for in SED fitting, since strong emission lines can affect IRAC fluxes. Selection of such galaxies is mostly contaminated by dusty starburst galaxies, with only little effect of nebular emission. While we do not have access to observational evidence of strong emission lines at this redshift, the $(3.6-4.5)\mu\text{m}$ color provide empirical evidence of strong $\text{H}\alpha$ emission, color reproduced consistently by our SED fitting tool. $\sim 20\%$ of our sample

identified as evolved galaxies at $z \sim 4$ is significantly affected by nebular emission, leading to younger ages, lower stellar masses, higher dust attenuation and higher SFRs. Complete results of this study are presented in Nayyeri et al. (2013).

We thank the SF2A organisers. SdB also thanks the SF2A for its financial support. SdB is supported by a Swiss National Science Foundation Early.Postdoc fellowship.

References

- Adelberger, K. L., Steidel, C. C., Shapley, A. E., et al. 2004, *ApJ*, 607, 226
- Anders, P. & Fritze-v. Alvensleben, U. 2003, *A&A*, 401, 1063
- Atek, H., Siana, B., Scarlata, C., et al. 2011, *ApJ*, 743, 121
- Bolzonella, M., Miralles, J., & Pelló, R. 2000, *A&A*, 363, 476
- Bruzual, G. & Charlot, S. 2003, *MNRAS*, 344, 1000
- Calzetti, D. 1997, *AJ*, 113, 162
- Calzetti, D., Armus, L., Bohlin, R. C., et al. 2000, *ApJ*, 533, 682
- de Barros, S., Schaerer, D., & Stark, D. P. 2012, *ArXiv e-prints*
- Erb, D. K., Shapley, A. E., Pettini, M., et al. 2006, *ApJ*, 644, 813
- Kashino, D., Silverman, J. D., Rodighiero, G., et al. 2013, *ArXiv e-prints*
- Labbe, I., Oesch, P. A., Bouwens, R. J., et al. 2012, *ArXiv e-prints*
- Lidman, C., Hayes, M., Jones, D. H., et al. 2012, *MNRAS*, 420, 1946
- Madau, P. 1995, *ApJ*, 441, 18
- McLinden, E. M., Finkelstein, S. L., Rhoads, J. E., et al. 2011, *ApJ*, 730, 136
- Nayyeri, H., Mobasher, B., Ferguson, H., et al. 2013, *ApJ*, submitted
- Oke, J. B., Cohen, J. G., Carr, M., et al. 1995, *PASP*, 107, 375
- Oke, J. B. & Gunn, J. E. 1983, *ApJ*, 266, 713
- Ono, Y., Ouchi, M., Shimasaku, K., et al. 2010, *ApJ*, 724, 1524
- Salpeter, E. E. 1955, *ApJ*, 121, 161
- Schaerer, D. & de Barros, S. 2009, *A&A*, 502, 423
- Schaerer, D. & de Barros, S. 2010, *A&A*, 515, A73+
- Schaerer, D. & de Barros, S. 2011, *ArXiv e-prints*
- Schaerer, D., de Barros, S., & Sklias, P. 2013, *A&A*, 549, A4
- Schenker, M. A., Ellis, R. S., Konidaris, N. P., & Stark, D. P. 2013, *ArXiv e-prints*
- Shim, H., Chary, R.-R., Dickinson, M., et al. 2011, *ApJ*, 738, 69
- Smit, R., Bouwens, R. J., Labbe, I., et al. 2013, *ArXiv e-prints*
- Stark, D. P., Schenker, M. A., Ellis, R., et al. 2013, *ApJ*, 763, 129
- Steidel, C. C., Adelberger, K. L., Shapley, A. E., et al. 2003, *ApJ*, 592, 728
- Steidel, C. C., Shapley, A. E., Pettini, M., et al. 2004, *ApJ*, 604, 534
- Trump, J. R., Impey, C. D., Kelly, B. C., et al. 2011, *ApJ*, 733, 60
- van der Wel, A., Straughn, A. N., Rix, H.-W., et al. 2011, *ApJ*, 742, 111